APPLICATION OF AVERAGE POSITIVE LYAPUNOV IN ESTIMATION OF CHAOTIC RESPONSE PEAK EXCITATION FREQUENCY OF HARMONICALLY EXCITED PENDULUM

Salau T. A.O. and Ajide O.O.
Department of Mechanical Engineering, University of Ibadan, Nigeria.

ABSTRACT

The fact that the drive parameters space of harmonically excited pendulum consist of mix parameters combination leading to different dynamics phenomena including chaotic and periodic responses is a strong motivation for this study aim at estimating the peak frequency that favour chaotic response. Simulation of pendulum and estimation of the average Lyapunov exponents by Grahm Schmidt Orthogonal rules at parameter nodal points selected from damp quality ($2.0 \le q \le 4.0$), excitation amplitude ($0.9 \le g \le 1.5$) and drive frequency ($0.5 \le \omega_D \le 1.0$) were effected using popular constant time step Runge-Kutta schemes (RK4, RK5 and RK5B) from two initial conditions through transient and steady periods. The impact of resolution on the measure of percentage of parameters combination leading to chaotic response (PPCLCR) was examined at resolution levels (R1 to R5) for increasing drive frequency. The validation cases were from those reported by Gregory and Jerry (1990) for ($\omega_D, q, g \equiv 2/3, 2, 1.5$) and ($\omega_D, q, g \equiv 2/3, 4, 1.5$) simulated from (0, 0) initial conditions. Corresponding validation results compare well with reported results of Gregory and Jerry (1990). The estimated peak frequency (0.6 radian /s) is the same across studied resolutions, initial conditions and Runge-Kutta schemes. The peak value of PPCLCR is 69.5, 69.4 and 69.4 respectively for RK4, RK5 and RK5B at initial conditions (0, 0). When initial conditions is (1, 0) the corresponding PPCLR value changes insignificantly to 69.6, 69.7 and 69.6 for RK4, RK5 and RK5B. Therefore affirms the utility and reliability of Lyapunov exponent as chaotic response identification tool.

I. INTRODUCTION

Lyapunov exponent otherwise known as characteristic exponent of dynamical systems has been described by Wikipedia (2013) as a quantity that characterises the rate of separation of infinitesimally close trajectories. There is no doubt that avalanche of relevant literature exists in the field of nonlinear dynamics in the last two decades on the usefulness of Lyapunov exponents as characterisation tool. The study of non-linear dynamic system behaviour using Lyapunov exponents is taking new interesting dimensions. The crucial role of Lyapunov exponents as tools for describing the behaviour of dynamic systems is enormous (Macro , 1996) .The author's paper demonstrated how numerical calculation of Lyapunov exponents can be used to analyze the stability of limits sets and check the presence of chaotic attractors. Mathematica software was used by the author to compute the Lyapunov spectrum of a smooth dynamic system. Detecting the presence of chaos in a dynamical system is an important problem that is solved by measuring the largest Lyapunov exponent. Michael *et al* (1993) in their paper demonstrated a practical method for calculating largest Lyapunov exponents from small data sets. The authors remarked that Lyapunov method follows directly from the definition of the largest Lyapunov exponent and is accurate because it takes advantage of all the available data. It has equally been shown in the paper that the Lyapunov based algorithm is fast, easy to implement, and robust to changes in embedding dimension, size of data set, reconstruction delay as well as noise level. In their paper, the versatility of Lyapunov exponent for detecting the manifestation of chaos in nonlinear dynamics has been clearly illustrated. Peter (1995) study focus on the development of model algorithm for the calculation of the spectrum of Lyapunov exponents that is generalised for system dynamics that are nonlinear. Souza-Machado *et al* (1990) has demonstrated how Lyapunov

exponents can be used to characterize deterministic chaos. This is adopted in a numerical experiment conducted by the author on the driven, damped, Duffing two-well oscillator. The paper stated that the results obtained affirm the importance of sum rule satisfied by the Lyapunov exponent spectra. It is concluded from the authors' paper that interesting, structure behaviour of the Lyapunov exponent spectra is observed as the duffing oscillator follows a pattern of periodic-doubling route to chaos. A study which explores a visualization technique on the basis of Mandelbrot set (M-set) methodology with the aim of an overall view of a chaotic system's dynamical performance in the parameter space has been carried out by Jin *et al* (2008). According to the author, the Lyapunov spectra with regard to different points in the parameter space were calculated. The points in the given parameter space were mapped to the computer screen and a colourful image named Lyapunov distribution map (LDM) was generated. The findings obtained from visualizing two typical chaotic systems have testified to the acceptability of this technique for visualization of chaotic systems. A study that investigated the characterisation of the dynamic responses of 3-dimensional Lorenz and Rösler models by Lyapunov's exponents has been carried out (Salau and Ajide, 2012). Popular but laborious Grahm Schmidt orthogonal rules were implemented for wider range of models driven parameters. It was established in the paper that estimation of Lyapunov's exponents' in Rösler model was found to be insensitive to algorithms due to its relative low degree of nonlinearity when compared with Lorenz model. The study also revealed that the sum of Lyapunov's spectrum is the same as the average of trace of variation square matrix over large iteration regardless of dependence on position variable or not. It can be concluded from the authors' findings that Lyapunov's exponents is a versatile characterising technique for dynamic systems response driven by different parameters combination. The objective of Changpin and Guarong (2004) paper was to determine both upper and lower bounds for all the Lyapunov exponents of a given finite-dimensional discrete map. The authors' work demonstrated significantly the efficiency of Lyapunov exponent estimation method for nonlinear system characterization. A novel methodology for forecasting chaotic systems which is based on exploiting the information conveyed by the local Lyapunov exponents of a system was developed by Dominique and Justin (2009). The outcome of the authors' study has been found to be a useful tool in correcting the inevitable bias of most non-parametric predictors. Non-stationary dynamical systems arise in applications, but little has been done in terms of the characterization of such systems using Lyapunov exponents (Ruth *et al*, 2008). This motivated Ruth et al in proposing a framework in 2008 for characterizing non-stationary dynamical systems using Lyapunov exponents and fractal dimension as tools. Through a well defined Lyapunov exponents and the fractal dimension based on a proper probability measure from the ensemble snapshots, the authors' findings revealed that the Kaplan-Yorke formula (one of the basic models in nonlinear dynamics) remains valid in most cases for non-stationary dynamical systems. Lyapunov exponents for chaotic systems for observed data evaluation in chaotic systems has been reviewed by Henry *et al* (1991). According to the authors, the exponents govern the growth or decrease of small perturbations to orbits of a dynamical system. It is understood from their paper that Lyapunov exponents are critical to the predictability of models made from observations as well as known analytic models. Lyapunov exponent has been widely accepted as a quantitative measure for the chaotic behaviour of dynamical systems. It is well known among researchers in this field that if the largest Lyapunov exponent is positive, it infers that the limit set is chaotic .Well established methods exist for the calculation of the spectrum of Lyapunov exponents for smooth dynamical systems. The main goal of Leine (2013) semester thesis was to investigate the relation between the synchronization property as well as the largest Lyapunov exponent of the system. The largest Lyapunov exponent is calculated using an approved method and is compared to the synchronization property of the coupled system. It is discovered from the study that the Lyapunov exponent is a reliable tool for chaos synchronization of mechanical systems. The analysis of chaotic systems has been done with the help of bifurcation diagrams and Lyapunov exponents (Archana *et al*, 2013).The qualitative changes in dynamics of the system were evaluated with the help of bifurcation diagrams. It is reported in the paper that for attractors of maps or flows, the Lyapunov exponents sharply separate between the different dynamics. According to the author, a positive Lyapunov exponent may be considered as the defining signature of chaos. Bifurcation diagrams are plotted and Lyapunov exponents are calculated for Lorenz and Rossler chaotic systems dynamics. The authors' article has again reinforced the utility of Lyapunov exponent as characterising tool for chaotic systems.

In the recent time , Salau and Ajide (2013) utilised positive Lyapunov exponents' criteria to develop chaos diagram on the parameters space of 4-dimensional harmonically excited vibration absorber control Duffing's Oscillator. Lyapunov's spectrum of modified Rösler system by constant time step fourth order Runge-Kutta method was found by the authors of this paper to compare correspondingly and qualitatively with what is reported in the literature.

Extensive literature search revealed that researches that adopted average positive Lyapunov in non-linear dynamics behaviour characterisation can be considered to be insignificant. The dearth of relevant literature that bothers on this is a strong motivation for the present paper. The objective of this paper is the application of average positive Lyapunov in the estimation of chaotic response peak excitation frequency of harmonically excited pendulum.

This article paper is divided into four sections. The introductory background of the study is given in section 1. Section 2 explains the methodology adopted for the study. Results and Discussion as well as conclusions are respectively provided in section 3 and section 4.

II. METHODOLOGY

Due to its engineering importance and its ability to exhibit rich nonlinear dynamics phenomena, harmonically excited pendulum has received extensive and continuous research interests as evident in the study by Gregory and Jerry (1990). In the non-dimensional and one dimensional form the governing equation of the damped, sinusoidally driven pendulum is given by equation (1). In this equation q is the damping quality parameter, g is the forcing amplitude, which is not to be confused with the gravitational acceleration, and ω_D is the drive frequency.

$$\frac{d^2\theta}{dt}+\frac{1}{q}\frac{d\theta}{dt}+\sin(\theta)=g\cos(\omega_D t) \tag{1}$$

Simulation of equation (1) with any of Runge-Kutta schemes demands its transformation under the assumptions ($\theta_1 = angular\ displacement$ and $\theta_2 = angular\ velocity$) to a pair of first order differential equations (2) and (3).

$$\dot{\theta}_1=\theta_2 \tag{2}$$

$$\dot{\theta}_2=g\cos(\omega_D t)-\frac{1}{q}\theta_2-\sin(\theta_1) \tag{3}$$

The present study employed the popular constant operation time step fourth order; fifth order and the Butcher's (1964) modified fifth order Runge-Kutta schemes to simulate equation (1) with equivalent first order rate equations (2) and (3). The respective details of each scheme are provided in equations (4) to (8); (9) to (15) and (16) to (22) substituting $y \leftarrow \theta_1, \theta_2, x \leftarrow t$ and constant time step h.

2.1 Fourth-Order Runge-Kutta Scheme

$$y_{i+1}=y_i+\frac{h}{6}\{K_1+2(K_2+K_3)+K_4\} \tag{4}$$

$$K_1=f(x_i,y_i) \tag{5}$$

$$K_2=f(x_i+\frac{h}{2},y_i+\frac{K_1 h}{2}) \tag{6}$$

$$K_3=f(x_i+\frac{h}{2},y_i+\frac{K_2 h}{2}) \tag{7}$$

$$K_4=f(x_i+h,y_i+K_3 h) \tag{8}$$

2.2 Fifth-Order Runge-Kutta Method

$$y_{i+1} = y_i + \frac{h}{90}\{7K_1 + 32K_3 + 12K_4 + 32K_5 + 7K_6\} \quad (9)$$

$$K_1 = f(x_i, y_i) \quad (10)$$

$$K_2 = f(x_i + \frac{h}{2}, y_i + \frac{K_1 h}{2}) \quad (11)$$

$$K_3 = f(x_i + \frac{h}{4}, y_i + \frac{(3K_1 + K_2)h}{16}) \quad (12)$$

$$K_4 = f(x_i + \frac{h}{2}, y_i + \frac{K_3 h}{2}) \quad (13)$$

$$K_5 = f(x_i + \frac{3h}{4}, y_i + \frac{(-3K_2 + 6K_3 + 9K_4)h}{16}) \quad (14)$$

$$K_6 = f(x_i + h, y_i + \frac{(K_1 + 4K_2 + 6K_3 - 12K_4 + 8K_5)h}{7}) \quad (15)$$

2.3 Butcher's (1964) Modified Fifth-Order Runge-Kutta Method

$$y_{i+1} = y_i + \frac{h}{90}\{7K_1 + 32K_3 + 12K_4 + 32K_5 + 7K_6\} \quad (16)$$

$$K_1 = f(x_i, y_i) \quad (17)$$

$$K_2 = f(x_i + \frac{h}{4}, y_i + \frac{K_1 h}{4}) \quad (18)$$

$$K_3 = f(x_i + \frac{h}{4}, y_i + (\frac{K_1}{8} + \frac{K_2}{8})h) \quad (19)$$

$$K_4 = f(x_i + \frac{h}{2}, y_i - \frac{K_2 h}{2} + K_3 h) \quad (20)$$

$$K_5 = f(x_i + \frac{3h}{4}, y_i + \frac{(3K_1 + 9K_4)h}{16}) \quad (21)$$

$$K_6 = f(x_i + h, y_i - \frac{(3K_1 - 2K_2 - 12K_3 + 12K_4 - 8K_5)h}{7}) \quad (22)$$

2.4 Solutions Schemes

The under-listed three distinct solution schemes were implemented in the present study.

- RK4-Constant **single** simulation time step fourth order Runge-Kutta scheme
- RK5-Constant **single** simulation time step fifth order Runge-Kutta scheme.
- RK5B-Constant **single** simulation time step Butcher's (1964) modified fifth order Runge-Kutta scheme.

2.5 Study Parameters

In tune with literature research interest this study focuses on the parameter plane defined by $2.0 \le q \le 4.0$ and $0.9 \le g \le 1.5$ investigated at different resolutions range from ten (10) to fifty (50) equal intervals each, and drive frequency $0.5 \le \omega_D \le 1.0$ examined in thirty (30) equal intervals with fixed simulation time step $h = \frac{T}{500}$ for excitation period ($T = 2\pi$). Two set of initial conditions (0, 0) and (1, 0) were investigated and the simulation was executed for 25-excitation periods including 10-periods of transient and 15-peiods of steady solutions.

The estimation of Lyapunov exponents was by Grahm Schmidt Orthogonal rules. The corresponding Runge-Kutta scheme effects the relevant transform functions associated with a unit length in orthogonal axes and Lyapunov exponents estimated at interval of ten simulation time steps and over the steady simulation periods. The average Lyapunov exponent is continuously estimated. At the end of total simulation periods the existence of at least one positive average Lyapunov exponent indicates chaotic response for the selected parameters.

III. Results and Discussion

Table 1 and figures 1 to 8 give validation results for the FORTRAN programmes developed for this study. Table 1 refers. The corresponding displacement and velocity components lack repetition with increasing number of completed excitation periods and across Runge-Kutta schemes. The Poincare patterns in figures 1 and 2 compare excellently well with those reported by Gregory and Jerry (1990) for respective damp quality of 2 and 4, excitation amplitude of 1.5 and drive frequency of $\frac{2}{3}$. Similarly the finite number of points in figures 3 and 4 affirms the periodic response results reported by Gregory and Jerry (1990) at damp quality of 2; drive frequency of $\frac{2}{3}$ and for respective excitation amplitude of 1.35 and 1.47. The corresponding variation of average Lyapunov exponents with increasing steady simulation periods are provided in figures 5 to 8 for the damp quality of 2 or 4, drive frequency of $\frac{2}{3}$ and respective excitation amplitude of 1.5, 1.5, 1.35 and 1.47.

Table 1: Sample steady simulated Poincare Solutions at excitation amplitude (1.5) and drive frequency ($\frac{2}{3}$).

No of excitation periods completed	q=2				q=4			
	RK4		RK5		RK4		RK5	
	θ_1	θ_2	θ_1	θ_2	θ_1	θ_2	θ_1	θ_2
1	-2.241	1.591	-2.241	1.591	2.194	-0.062	2.183	-0.070
2	-0.588	2.277	-0.588	2.277	1.715	2.365	2.909	0.788
3	1.076	1.944	1.076	1.944	1.324	2.221	2.910	0.578
4	-2.450	1.438	-2.450	1.438	-0.449	2.804	-0.825	0.772
5	2.521	0.431	2.521	0.431	-1.280	2.058	-0.283	2.838
6	-2.750	1.217	-2.750	1.217	-0.600	0.760	-0.487	1.690
7	0.343	0.278	0.343	0.278	-2.898	0.982	0.698	-0.278
8	-0.011	1.426	-0.011	1.426	1.722	1.850	1.870	-0.238
9	-2.616	1.283	-2.616	1.283	-0.976	2.130	-0.081	-0.363
10	0.607	0.067	0.606	0.068	-0.658	0.861	1.909	-0.240
11	0.001	1.380	0.001	1.380	-1.637	2.229	-0.076	-0.374
12	2.103	0.190	2.104	0.191	-0.617	0.709	1.934	-0.224
13	0.787	2.226	0.893	2.171	0.655	-0.476	-0.026	-0.414
14	-2.644	1.298	-2.961	1.054	2.717	0.358	2.040	-0.156
15	0.619	0.061	0.149	0.559	-1.200	1.565	1.268	-0.585

16	0.001	1.378	-0.028	1.443	1.826	-0.032	3.025	0.621
17	2.064	0.170	-2.086	1.664	0.610	-0.650	-0.170	-0.071
18	0.074	1.400	-0.034	2.176	-2.912	0.897	1.479	-0.470
19	-2.909	1.060	1.012	2.020	1.872	1.776	1.696	-0.319
20	0.157	0.541	-2.382	1.494	-0.475	1.612	0.279	-0.501

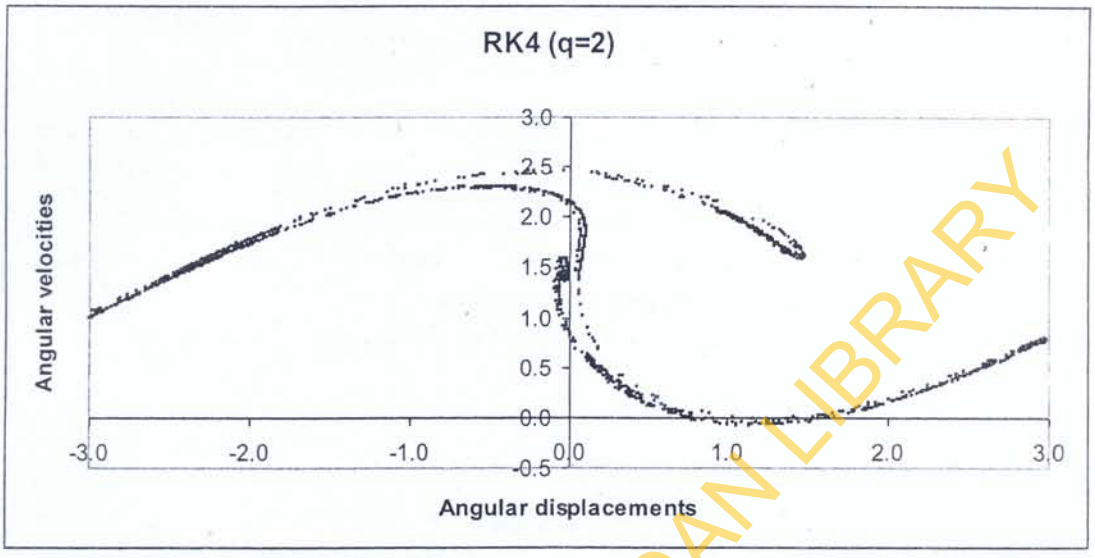

Figure 1: Poincare section of harmonically excited pendulum by RK4 and for q=2, g=1.5 and $\omega_D = \frac{2}{3}$.

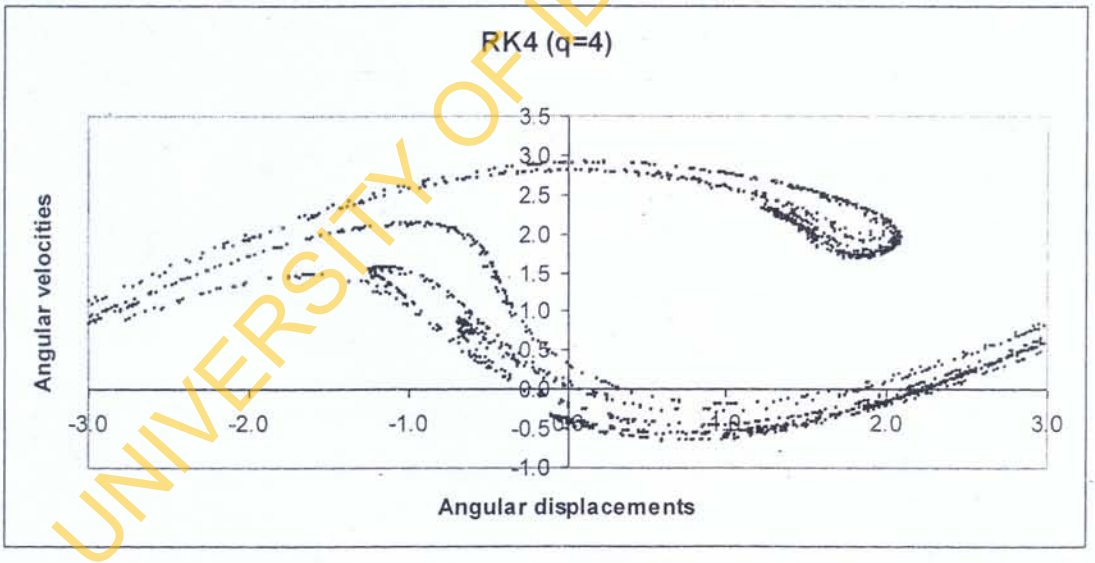

Figure 2: Poincare section of harmonically excited pendulum by RK4 and for q=4, g=1.5 and $\omega_D = \frac{2}{3}$.

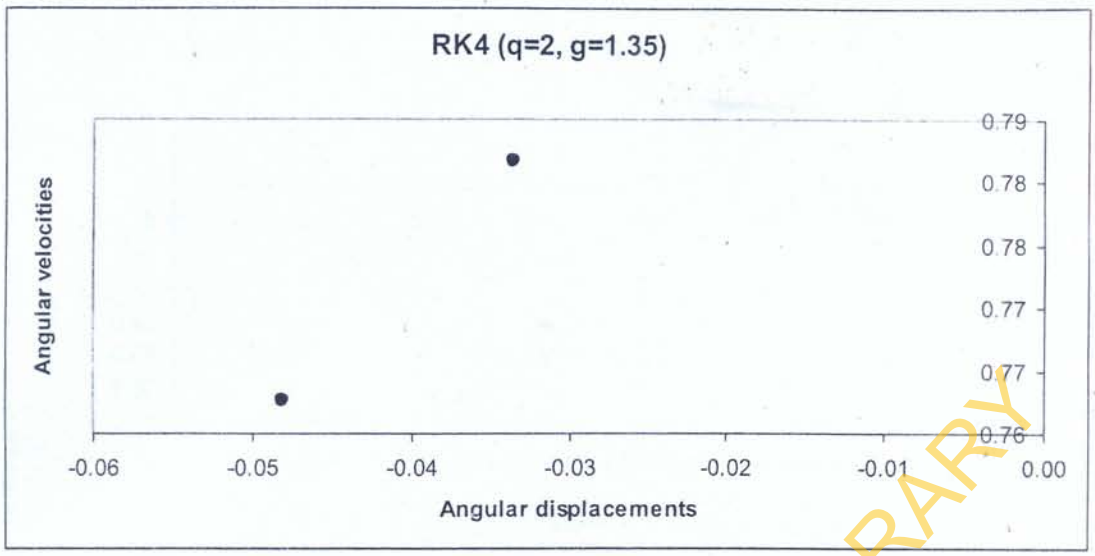

Figure 3: Poincare section of harmonically excited pendulum by RK4 and for q=2, g=1.35 and $\omega_D = \frac{2}{3}$

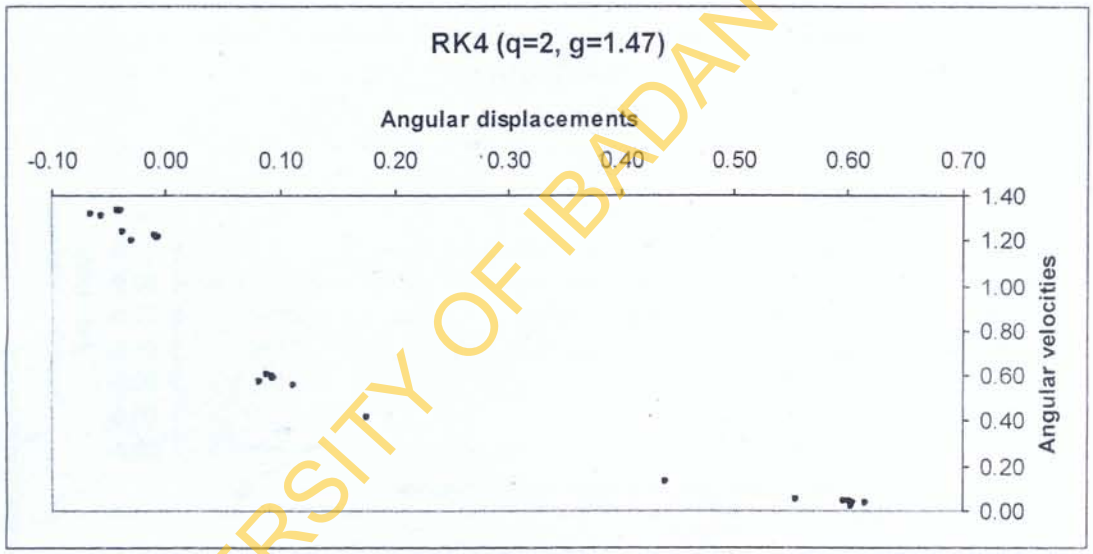

Figure 4: Poincare section of harmonically excited pendulum by RK4 and for q=2, g=1.47 and $\omega_D = \frac{2}{3}$

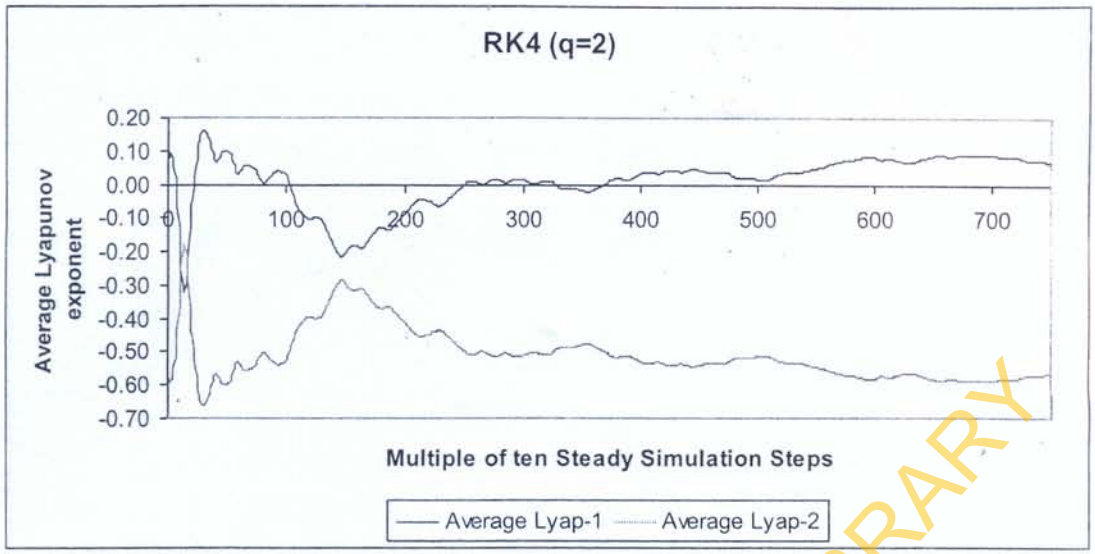

Figure 5: Variation of average Lyapunov exponents along two orthogonal directions of harmonically excited pendulum by RK4 and for q=2, g=1.5 and $\omega_D = \frac{2}{3}$.

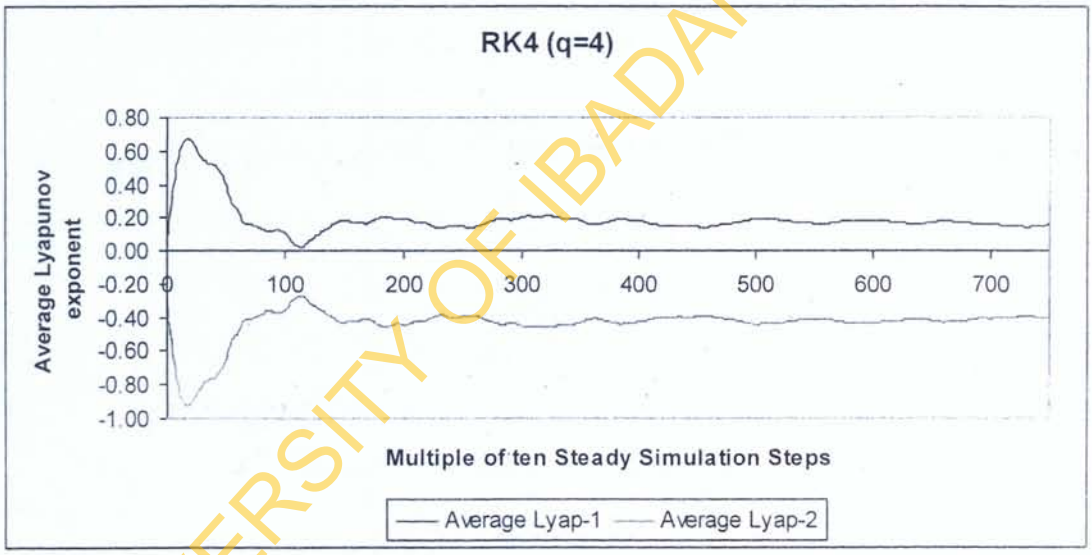

Figure 6: Variation of average Lyapunov exponents along two orthogonal directions of harmonically excited pendulum by RK4 and for q=4, g=1.5 and $\omega_D = \frac{2}{3}$.

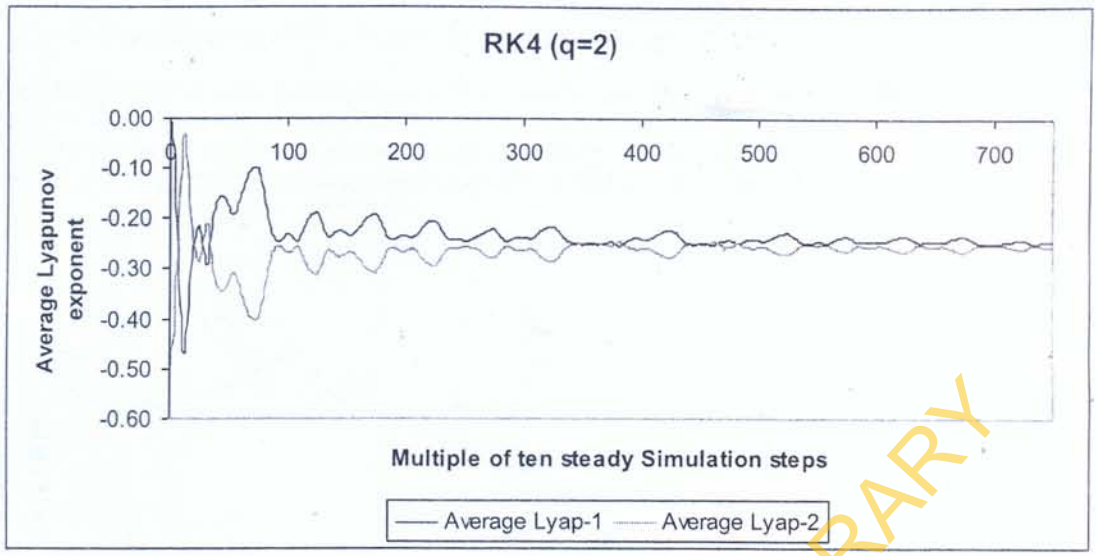

Figure 7: Variation of average Lyapunov exponents along two orthogonal directions of harmonically excited pendulum by RK4 and for q=2, g=1.35 and $\omega_D = \frac{2}{3}$.

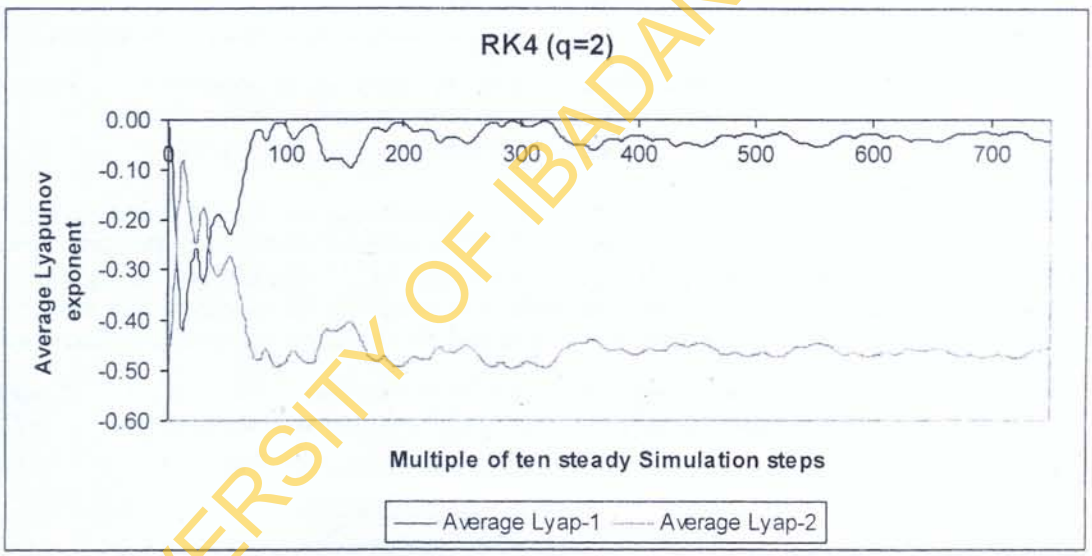

Figure 8: Variation of average Lyapunov exponents along two orthogonal directions of harmonically excited pendulum by RK4 and for q=2, g=1.47 and $\omega_D = \frac{2}{3}$.

Figures 1 to 8 refer. Each Poincare section compare well in quality with the corresponding result reported by Gregory and Jerry (1990). In addition the existence of at least one average positive Lyapunov exponent as illustrated respectively in figures 5 and 6 affirm the chaotic response at damp quality of 2 and 4 respectively and excitation amplitude of 1.5 and drive frequency of $\frac{2}{3}$. Similarly non-existence of at least one average positive Lyapunov exponent as illustrated respectively in figures 7 and 8 affirm the periodic response at damp quality of 2, respective excitation amplitude of 1.35 and

1.47 and drive frequency of $\frac{2}{3}$. In addition the visual assessment of the Poincare sections shows that the filling of the phase space increases with increasing damping quality and vice versa while keeping other driven parameters constant.

Figure 9 presented the results of variation of percentage of parameters combination leading to chaotic response (**PPCLCR**) for increasing resolution (R1 to R5) and drive frequency

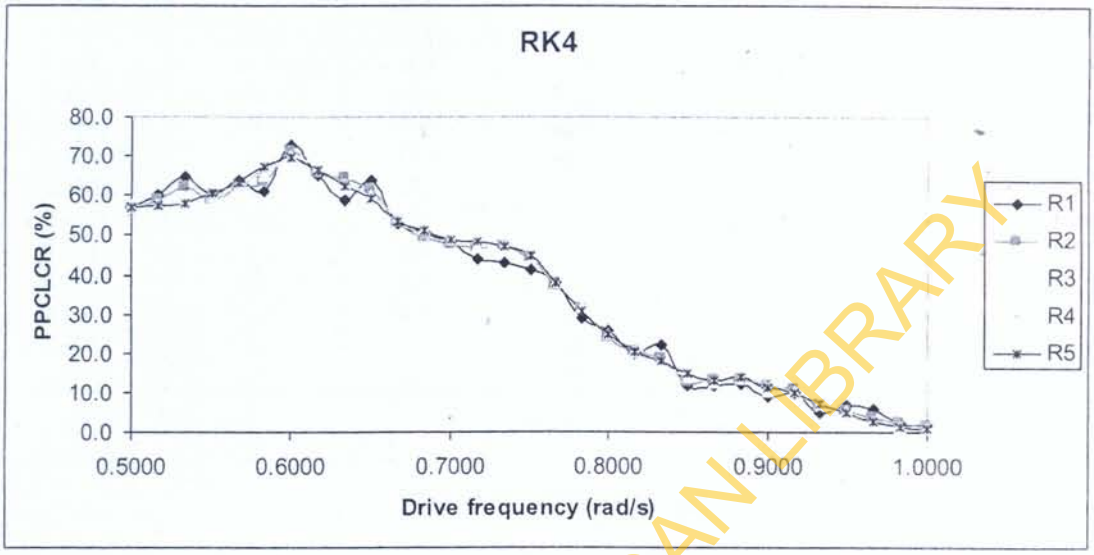

Figure 9: Variation of percentage of drive parameters combination leading to chaotic response (PPCLCR) of harmonically excited pendulum by RK4 and for initial conditions (0, 0), $2 \le q \le 4$, $0.9 \le g \le 1.5$ and $0.5 \le \omega_D \le 1.0$.

Figure 9 refers. Though not significantly high the accuracy of variation of percentage of drive parameters leading to chaotic response (PPCLCR) of harmonically excited pendulum improve with increasing resolution from R1 (11×11 grid points) to R5 (51×51 grid points) at constant step of ten (10). The peak frequency for all studied resolutions is 0.6 radian/s. The PPCLCR decreases slowly below peak frequency and rapidly toward zero in at drive frequency of one (1).

Table 2: Quantitative comparison of variation of percentage of drive parameters combination leading to chaotic response (PPCLCR) of harmonically excited pendulum for $2 \le q \le 4$, $0.9 \le g \le 1.5$ and $0.5 \le \omega_D \le 1.0$.

Drive frequency	RK4		RK5		RK5B	
	PPCLCR (%) for two Initial Conditions					
	(0, 0)	(1, 0)	(0, 0)	(1, 0)	(0, 0)	(1, 0)
0.5000	56.9	55.6	56.6	55.7	56.5	55.7
0.5167	57.4	57.6	57.6	57.5	57.6	57.6
0.5333	57.8	58.4	57.7	58.2	57.7	58.3
0.5500	60.7	59.7	60.9	59.9	61.0	59.8
0.5667	63.1	62.2	63.0	62.2	62.9	62.3
0.5833	67.2	65.8	67.3	65.9	67.3	65.8
0.6000	69.5	69.6	69.4	69.7	69.4	69.6
0.6167	66.5	66.3	66.5	66.5	66.6	66.6
0.6333	62.5	63.3	62.6	63.4	62.5	63.4
0.6500	59.3	59.8	59.4	59.7	59.4	59.8
0.6667	53.2	54.4	53.2	54.3	53.2	54.2
0.6833	50.9	51.2	50.8	51.1	50.8	51.1

0.7000	48.8	49.9	48.7	49.8	48.8	49.7
0.7167	48.2	48.2	48.2	48.1	48.2	48.0
0.7333	47.2	47.9	47.3	47.9	47.3	48.1
0.7500	44.6	45.3	44.7	45.4	44.6	45.4
0.7667	38.1	38.8	38.1	38.9	38.0	38.8
0.7833	30.9	31.1	30.9	31.1	31.0	31.1
0.8000	24.9	26.3	24.9	26.4	24.9	26.2
0.8167	20.1	21.8	20.0	21.8	20.0	21.8
0.8333	17.9	18.8	17.9	19.0	18.0	19.0
0.8500	14.7	15.9	14.6	15.9	14.6	15.9
0.8667	13.2	14.0	13.2	14.2	13.3	14.2
0.8833	14.1	13.5	14.1	13.5	14.1	13.5
0.9000	11.5	12.0	11.4	12.1	11.3	12.3
0.9167	10.0	9.0	10.1	9.2	10.1	9.2
0.9333	7.4	6.8	7.3	6.8	7.3	6.9
0.9500	5.0	5.9	4.9	5.9	4.9	5.9
0.9667	2.7	4.2	2.7	4.2	2.7	4.2
0.9833	1.6	2.1	1.5	2.2	1.5	2.3
1.0000	0.9	1.0	0.9	1.0	0.9	1.0

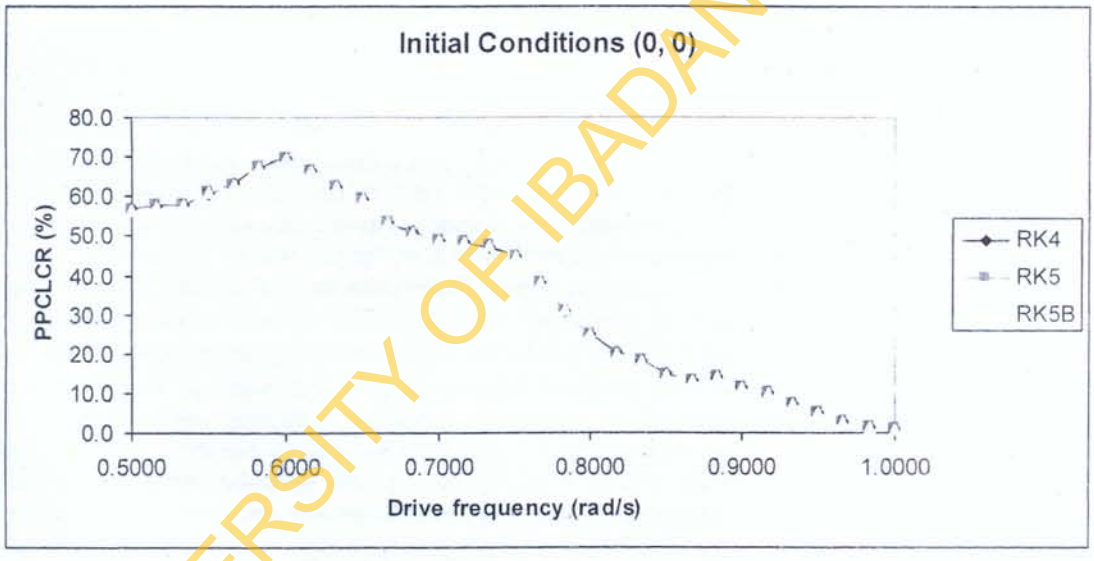

Figure 10: Variation of percentage of drive parameters combination leading to chaotic response (PPCLCR) of harmonically excited pendulum by RK4 and for initial conditions (0, 0), $2 \le q \le 4$, $0.9 \le g \le 1.5$ and $0.5 \le \omega_D \le 1.0$.

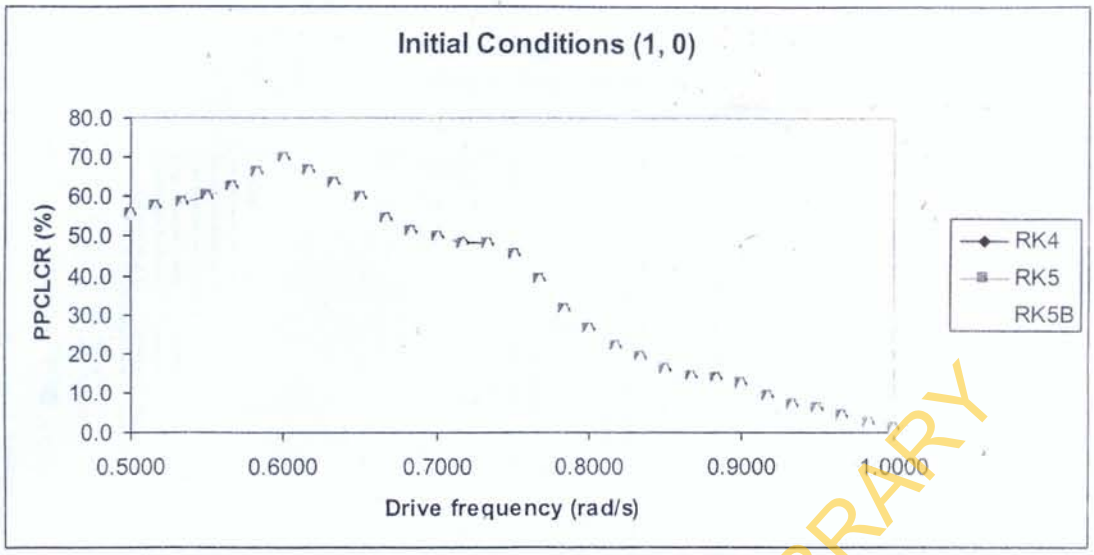

Figure 11: Variation of percentage of drive parameters combination leading to chaotic response (PPCLCR) of harmonically excited pendulum by RK4 and for initial conditions (1, 0). $2 \le q \le 4$, $0.9 \le g \le 1.5$ and $0.5 \le \omega_D \le 1.0$.

Table 2 and figures 10 and 11 refer. The peak frequency is 0.6 radian/s for all the cases of initial conditions and Runge-Kutta schemes studied. The peak value of PPCLCR is 69.5, 69.4 and 69.4 respectively for RK4, RK5 and RK5B at initial conditions (0, 0). However when the simulation initial conditions is (1, 0) the corresponding PPCLR value changes insignificantly to 69.6, 69.7 and 69.6 for RK4, RK5 and RK5B. In addition there is no significant difference in PPCLR value across initial conditions and schemes with increasing level of drive frequency.

Figure 12 presented the chaos diagram at peak frequency simulated form initial conditions (0, 0) and using constant step fourth order Runge-Kutta (RK4) scheme. The estimation of the average Lyapunov exponents by Grahm Schmidt Orthogonal rules was effected along two perpendicular axes at 51×51 grid points on the driven parameters plane defined by $2 \le q \le 4$ and $0.9 \le g \le 1.5$. The set of scatter plots in figure 12 identified drive parameters combination leading to chaotic response of the harmonically driven pendulum supported by evidence of at least one average positive Lyapunov exponent. The pendulum responded chaotically at a total of 1808 parameters combination out of 2601 maximum possible, which is the same as PPCLCR of 69.5 obtained at peak frequency. Periodic response of the pendulum can be obtained at driven parameters combination selected in the blank regions of figure 12.

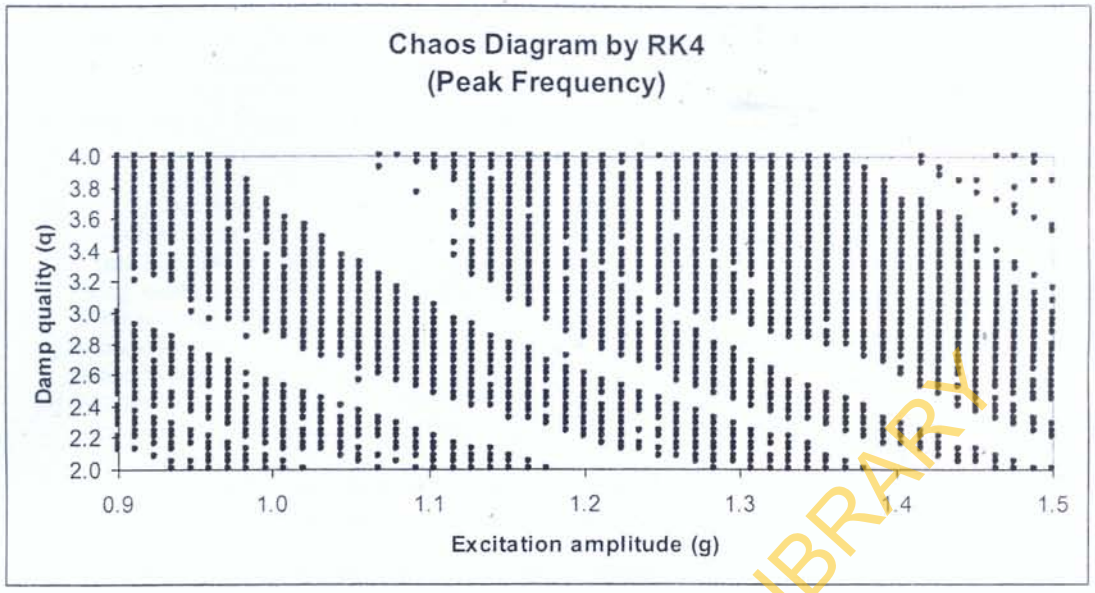

Figure 12: Chaos diagram on the drive parameters plane ($2 \le q \le 4$ and $0.9 \le g \le 1.5$) with 51×51 grid points and at peak frequency (0.6radian/s) of harmonically excited pendulum by RK4 and for initial conditions (0, 0).

IV. CONCLUSIONS

This study utilised average positive Lyapunov exponent criteria estimated by Grahm Schmidt Orthogonal rules to determine the peak frequency of harmonically excited pendulum. The peak frequency is the drive frequency at which the percentage of drive parameters combination leading to chaotic response (PPCLCR) is highest over a range of studied drive frequency. The estimated peak frequency (0.6 rad. /s) is the same across studied resolutions, initial conditions and Runge-Kutta schemes. Therefore the utility of Lyapunov exponent as chaotic response identification tool reaffirmed.

V. FUTURE APPLICATIONS

Some of the future applications of this study included the under-listed.

- The results of the present study can be employed to select suitable drive frequency in addition to other driven parameters that will guarantee chaotic behaviour of harmonically driven nonlinear pendulum.
- The platform developed in the present study is a versatile diagnosing tool for distinguishing dynamic behaviour of dynamic systems such as nonlinear pendulum, Duffing oscillator etc. Their behaviour can be classified as periodic or quasi-periodic or chaotic.
- With little modifications the platform can be adapted to similarly investigate higher order or higher dimensional dynamic systems such as Lorenz, Rossler etc.

REFERENCES

[1]. Archana R., Unnikrishman A. and Gopikakumari R. (2013), Bifurcation analysis of chaotic systems using a model built on artificial neural networks, 2nd International conference on computational techniques and artificial intelligence (ICCTAI'2013), March 17-18, 2013, Dubai (UAE).

[2]. Changpin Li. and Guarong C. (2004), Estimating the Lyapunov exponent of discrete systems. American Institute of Physics: Chaos- An Interdisciplinary Journal of Nonlinear Science, Vol.14, Issue 2. http://dx.doi.org/10.1063/1.1741751.

[3]. Dominique G. And Justin L. (2009), Forecasting chaotic systems: The role of local Lyapunov exponents. Chaos, Solitons and Fractals, Vol.41 (5). DOI: 10.1016/j.chaos.2008.09.017
[4]. Gregory L. B. and Jerry P. G. (1990), chaotic dynamics: An Introduction, Cambridge University Press. USA, pp.3-5 & 40-75.
[5]. Henry D.I.A., Reggie B. And Kennel M.B. (1991), Lyapunov exponents in chaotic systems: Their importance and their evaluation using observed data. International Journal of Modern Physics B, Vol.5, Issue 09. DOI : 10.1142/s021797929100064X
[6]. Jin C., Jiantrong and Chunbiao T. (2008), Visualisation of chaotic dynamic systems Based on Mandelbrot set methodology. Fractals, Vol.16, Issue 1. DOI : 10.1142/S0218348X08003752
[7]. Leine R.I. (2013), Determining the largest Lyapunov exponent of mechanical systems with impacts using chaos synchronisation. A semester thesis at the institute of Mechanical systems, centre of Mechanics, Zurich.
[8]. Macro S. (1996), Numerical calculation of Lyapunov exponents. The MATHEMATICA Journal, Miller Freeman publications.
[9]. Michael T.R.,James J.C. and Carlo J.D. (1993), A practical method for calculating largest Lyapunov exponents from small data sets. Physica D, Vol.65, pp.117-134, Elsevier science publishers. SDI: 0167-2789(92)00033-6.
[10]. Peter C.M. (1995), Calculation of Lyapunov exponents for dynamical systems with discontinuities. Some Nonlinear Oscillations Problems in Engineering Sciences, Elsevier Journal,Vol .5, Issue 9,pp.1671-1681.
[11]. Ruth S.,Ying-Cheng L. and Qingfei C.(2008), Characterisation of non-stationary chaotic systems. American Physical Society (APS) Journal, Physical Review E, Vol. 77, Issue 2. http:link.aps.org/doi/10.1103/PhysRevE.77.026208.
[12]. Salau T.A.O. and Ajide O.O. (2012), Simulation and Lyapunov exponent characterisation of Lorenz and Rosler dynamics. International Journal of Engineering and Technology (IJET), Vol. 2, No.9. ISSN: 2049-3444.
[13]. Salau T.A.O. and Ajide O.O. (2013), Chao diagrams of harmonically excited vibration absorber control duffing oscillator. International Journal of Scientific and Engineering Research, Vol. 4, Issue 1 (8 pages).
[14]. Souza-Machado S.D., Rollins R.W., Jacobs D.T. and Hartman J.L. (1990), Studying chaotic system using microcomputer simulations and Lyapunov exponents. American Journal of Physics, Vol.58 (4), pp.321-329. American Association of Physics Teachers.
[15]. Steven C. C. and Raymond P. C. (2006), Numerical methods for engineers, Fifth edition, McGraw-Hill (International edition), New York, ISBN 007-124429-8.
[16]. Wikipedia (2013), Lyapunov exponents. Downloaded on Friday, 31st May 2013 from http://en.wikipedia.org/wiki/Lyapunov_exponent.

APPENDIX-I:

Simulation procedures (set-up)

(1) START
(2) Read Basic common parameters including the initial conditions from the input file.
(3) Select Runge-Kutta Scheme (Fourth order or Fifth order or Butcher's (1964) modified fifth order).
(4) Select the First or the second initial conditions.
(5) Select the First or the Next resolution
(6) Select the First or the Next drive frequency (ω_D).
(7) Select the First or the Next Parameter point (q, g) and **set** or **reset** the initial conditions as appropriate for the simulation of the pendulum and Lyapunov value estimation.
(8) Use constant time step Runge-Kutta scheme to simulate both unsteady and steady solutions of nonlinear and harmonically excited pendulum (governing equation expressed as first order rate). Simultaneously and for each time step employ Grahm Schmidt Orthogonal rules (coded according to selected Runge-Kutta scheme) to sequentially effect the transformation of a unit radius circle to its corresponding elliptic shape. After ten (10) consecutive time steps within the steady solutions region estimate the local Lyapunov values and track results (for further processing), then renormalize ellipse to a unit radius circle. Repeat the estimation of the local Lyapunov values for as long as steady simulation of the pendulum lasted while tracking relevant simulation results.
(9) Evaluate the average of the estimated local Lyapunov value along the angular displacement and angular velocity axes. Keep the census if the sign of the greater of the average Lyapunov values is positive for